

# Design Studies and Performance of Single-Phase HEFSM with Various Rotor Pole Number for Hybrid Electric Vehicle Applications

Mohamed Mubin Aizat Mazlan, Md Zarafi Ahmad,  
Syed Mohammad Naufal Syed Othman and Erwan Sulaiman  
Department of Electrical Power Engineering  
Universiti Tun Hussein Onn Malaysia, Locked Bag 101  
Batu Pahat, Johor, 86400 Malaysia  
mubinaizat@gmail.com and erwan@uthm.edu.my

**Abstract**—Recently, many researchers have developed hybrid excitation flux switching machine (HEFSM) for HEV applications. The designed HEFSM consist of permanent magnet (PM) and field excitation coil (FEC) as their main flux sources. HEFSM also consist a robust rotor structure. However most of the designed HEFSM used three-phase winding. Three-phase winding are complicated and has high copper losses. As one of alternative, a new design of single-phase hybrid excitation flux switching motor (HEFSM) for direct drive HEV is proposed. In this paper, the performance comparison of single-phase hybrid excitation flux switching machine with various rotor pole numbers is analysed. The flux comparison of PM with DC FEC, flux linkage at various FEC current densities,  $J_E$ , cogging torque, Induced voltage/ back EMF of PM with DC FEC, torque and power versus FEC current density,  $J_E$  at various armature coil current densities,  $J_A$  are investigated. The generated results show that the appropriate combination of stator slot-rotor pole configurations are 8S-4P and 8S-8P respectively, which initially provide highest power and torque performance. Therefore, by further design modification and optimization it is expected that the low cost motor will successfully achieved the target performances.

**Index Terms**—Hybrid Excitation Flux Switching Motor, Hybrid Electric Vehicle and Single-Phase Winding

## I. INTRODUCTION

By increasing number of population in the world, the demand toward vehicles for personal transportation has also been increased dramatically in the past of decade which leads to serious problems called ‘global warming’. One of the main causes of global warming is Internal Combustion Engine (ICE). Through the report in year 2008 [1], about seven per cent of global carbon dioxide (CO<sub>2</sub>) emission in year 2000 came from the vehicles. By the year 2015, it is expected that CO<sub>2</sub> emission rate from vehicles will increase two times with economic growth.

Hybrid Electric Vehicle (HEV) is considered as an ultimate eco- friendly car and this is highly expected to be popularized in the future [2]. The important of the basic characteristics requirements of an electric motor for HEV drive systems are high torque, high power density, and constant power at high speed as well as high efficiently [3].

Fig. 1 illustrated the main candidates of electric machine for HEV drive. Permanent Magnet Synchronous Machine (PMSMs) is used in HEV to overcome problem of low torque density and efficiency [4]. Although PMSM has the advantage of high torque density and high efficiency, still it has the problem of demagnetization and mechanical damage of rotor’s magnet. Due to this reason, other alternative machine should be design to overcome the problems of PMSM already installed in HEV.

DC motors have been widely accepted in electric propulsion due to use battery as DC supply and simple control principle. However, DC motor drives have a few disadvantages such as low reliability, unstable current and high maintenance [5]. Thus DC motors are unsuitable for maintenance-free drives.

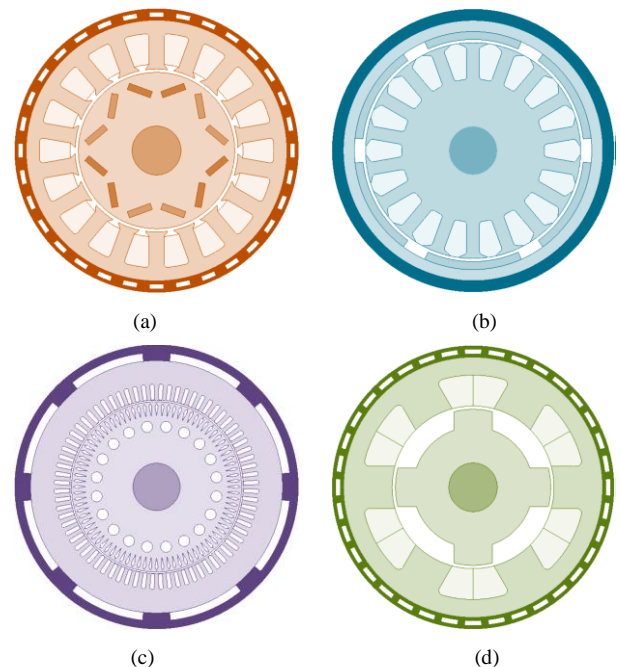


Fig. 1. Four Main Candidates of Electric Machine for HEV Drive  
(a) Permanent Magnet Synchronous Machines (b) DC motor

(c) Induction Motor (d) Switched Reluctant Motor

At present, induction motor (IM) are generally established as the most potential candidate for the electric propulsion of HEVs, due to their reliability, ruggedness, low maintenance, and low cost [6]. However, IM drives have demerits such as high loss, low efficiency and low power factor [7].

Then switched reluctance motor (SRM) is invented to overcome the permanent magnet problem. SRM has no PM and robust rotor structure but it is not suitable for HEV due to large torque ripples and noisy [8].

On the other hand, permanent magnet flux switching machine (PMFSM) has been proposed. This PMFSM has physical compactness, robust rotor structure, higher torque and power density and high efficiency. All magnets are located at the stator which make the temperature of the magnet can easily be controlled [9]. This shows that PMFSM have more advantage when compared with PMSM and SRM [10-12]. The application such as in aircrafts, automotive traction drives, and wind power generation are widely used by using PMFSM, [13-14]. However PMFSM has several disadvantages of uncontrolled flux and high cost.

Recently, many researchers have developed hybrid excitation flux switching machine (HEFSM) for HEV applications. There are two main flux sources which are permanent magnet (PM) and field excitation coil (FEC). These HEMs have better features when compared with interior permanent magnet synchronous machines (IPMSM) used in conventional hybrid electric vehicles (HEVs). Since all flux sources including PM, FEC and armature coils are located on stator core, the rotor becomes a single piece structure similar with switch reluctance machine (SRM). The combined flux generated by PM and FEC established more excitation fluxes that are required to produce much higher torque of the motor. In addition, variable DC FEC can control the flux capabilities of the motor, thus the machine can be applied for high-speed motor drive system.

Several invention of HEFSM for HEV application has been proposed. For example some, 6Slot-5Pole HEFSSM for HEV application has been proposed. Although the proposed machine has met the target performances, the problem of unbalanced pulling force due to odd number of poles is difficult to overcome [15-16]. Besides, 6Slot-8Pole machines also had been proposed but these types of machines have problems of high torque ripple and back-emf waveforms, which are usual concerns for this kind of eight pole machine [17]. It should be noted that all HEFSM mentioned above are 3-phase HEFSM.

Due to complicated winding and high copper losses of 3-phase HEFSM, a simple structure of single-phase HEFSM is proposed in which the copper losses will reduce and efficiency will increase. In this paper, the impact of rotor pole number of the proposed motor with 8 stator slots is investigated in this paper in order to determine the optimal performances. Then flux comparison of PM with DC FEC, flux linkage at various FEC current densities,  $J_E$ , cogging torque, Induced voltage/back EMF of PM with DC FEC, torque and power versus FEC current density,  $J_E$  at various armature coil current densities,  $J_A$  are also analyzed.

## II. OPERATING PRINCIPLE OF HEFSM

The term “flux switching” is introduced due to the changing of the polarity of the flux linkage by following the motion of salient pole rotor. In the proposed HEFSM, the possible number of rotor pole and stator slot is defined by (1)

$$N_r = N_s (1 \pm \frac{k}{2q}) \quad (1)$$

Where  $N_r$  is the rotor poles number,  $N_s$  is the number of stator slots,  $q$  is the number of phases and the natural number is defined as  $k$ . For the proposed motor,  $q$  is set as single phase,  $N_s$  is set as 8 and  $N_r$  are set 4, 8, 12, 16, and 20. In general, the rotation frequency of mechanical,  $f_m$  and the frequency of electrical,  $f_e$  for the proposed motor can be articulated as (2), where  $f_e$ ,  $N_r$  and  $f_m$  is the frequency of electrical, number of rotor poles and mechanical rotation frequency, respectively.

$$f_e = N_r f_m \quad (2)$$

The operating principle of OR-HEFSM is demonstrated in Fig. 2. The red line indicates flux from PM and blue line indicates the flux from FEC, respectively. In Fig. 2(a) and (b), the polarity of both red and blue indicator are in the same direction. Thus, both of the PM and FEC fluxes are merged and flow together into the rotor. The combination of both fluxes generated more fluxes and called hybrid excitation flux. While in Fig 2(c) and (d), where the blue indicator is in reverse polarity and flow around the stator yoke, only the red indicator of PM flux flows into the rotor which results in less flux excitation.

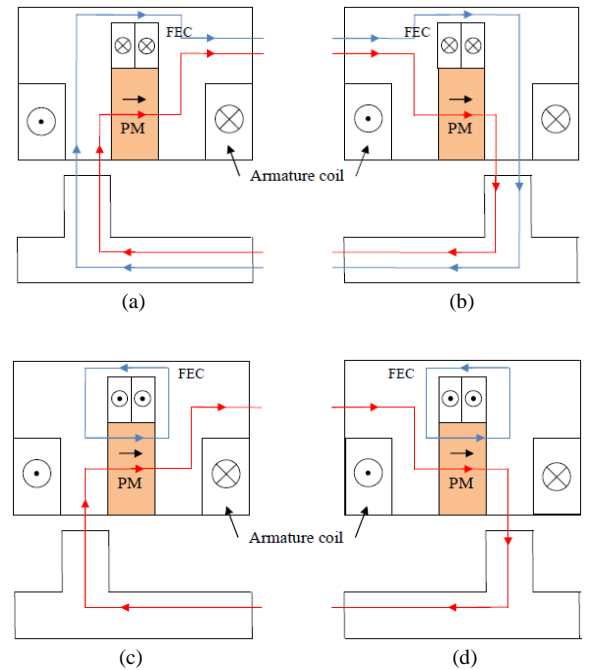


Fig. 2. Principle Operation of Outer-rotor HEFSM (a)  $\theta_e = 0^\circ$  (b)  $\theta_e = 180^\circ$  more excitation, (c)  $\theta_e = 0^\circ$  (d)  $\theta_e = 180^\circ$  less excitation

### III. DESIGN RESTRICTIONS, SPECIFICATIONS AND PARAMETERS OF OR-HEFSM

Table I shows the electrical restrictions related with the inverter such as maximum 375V DC bus voltage and maximum 360A inverter current are set. The limits of the current densities are set to the maximum of  $30A_{rms}/mm^2$  and  $30A/mm^2$  for armature winding and DC FEC, respectively. In addition, the geometrical dimensions of the HEFSM such as the stator outer diameter, motor stack length, shaft radius and air gap are set to 264mm, 70mm, 30mm and 0.8mm respectively, while the PM weight is set to be 1.0kg. The target performance for maximum torque and power are 111Nm and 41kW respectively.

The commercial FEA package, JMAG-Designer ver.13.0, released by Japan Research Institute is used as 2D-FEA solver in this design. The material used for PM is NEOMAX 35AH with residual flux density and coercive force at 20 ° are 1.2T and 932 kA/m respectively. Whereas for the stator and rotor body, the material used is electrical steel, 35H210.

Table II shows the parameters of HEFSM. From Table II, the rotor parameters involved are the outer rotor radius ( $D_1$ ) which is 70% of the size of motor and within the range of general machine split ratio, rotor pole depth ( $D_2$ ) which is half size of the rotor and to ensure flux moves from stator to rotor equally without any flux leakage, the design of rotor pole arc width ( $D_3$ ) is defined as in (3). It is to allow optimal flux flows into the rotor pitch. The rotor pole width is decrease when the number of pole increases.

$$\sum W_s = \sum W_r \quad (3)$$

The distance between airgap and PM is ( $D_4$ ). The PM slot shape parameters are the PM depth ( $D_5$ ), and the PM width ( $D_6$ ) calculated by using volume of 1kg PM. The size of  $D_5$  is one third of the stator expecting will give more flux to flow and increase the motor performances while for the FEC slot depth and FEC slot width, ( $D_7$ ) and ( $D_8$ ) calculated from (4). The FEC slot width is one third of the stator and expecting the flux have enough space to flow easily.

$$N_a = \frac{J_a \alpha S_a}{I_a} \quad (4)$$

Finally, the armature coil parameters are armature coil slot depth ( $D_9$ ) and the armature coil slot width ( $D_{10}$ ) calculated from (5) by using 168mm area of armature coil. Therefore, the depth of  $D_9$  is two third of the stator and will prevent flux saturation and make the flux easily through it.

$$N_e = \frac{J_e \alpha S_e}{I_e} \quad (5)$$

The motor design parameters, from  $D_1$  to  $D_{10}$  are demonstrated in Fig. 3. Then the initial design of the machine configurations of 8 stator slots of various rotor pole numbers is illustrated as in Fig. 4. The machine windings are the same for all rotor pole number configurations.

TABLE I  
HEFSM DESIGN RESTRICTIONS

Items	Unit	HEFSM
Max. DC-bus voltage inverter	V	375
Max. inverter current	$A_{rms}$	360
Max. current density in armature winding, $J_a$	$A_{rms}/mm^2$	30
Max. current density in excitation winding, $J_e$	$A/mm^2$	30
Stator outer diameter	mm	264
Motor stack length	mm	70
Shaft radius	mm	30
Air gap length	mm	0.80
PM weight	kg	1
Maximum torque	Nm	>111
Maximum power	kW	>41

TABLE II  
DESIGN PARAMETER OF HEFSM

Parameter	Description	HEFSM
$D_1$	Rotor outer radius (mm)	92.40
$D_2$	Rotor pole depth (mm)	31.20
$D_3$	Rotor pole width (mm)	varies
$D_4$	Distance of airgap (mm)	0.80
$D_5$	PM depth (mm)	12.55
$D_6$	PM width (mm)	8.86
$D_7$	FEC slot depth (mm)	13.35
$D_8$	FEC slot width (mm)	10.99
$D_9$	AC slot depth (mm)	26.70
$D_{10}$	AC slot width (mm)	6.29
Area of FEC ( $mm^2$ )		147.67
Area of armature coil ( $mm^2$ )		144
FEC coil number (turns)		44
Armature coil number (turns)		7

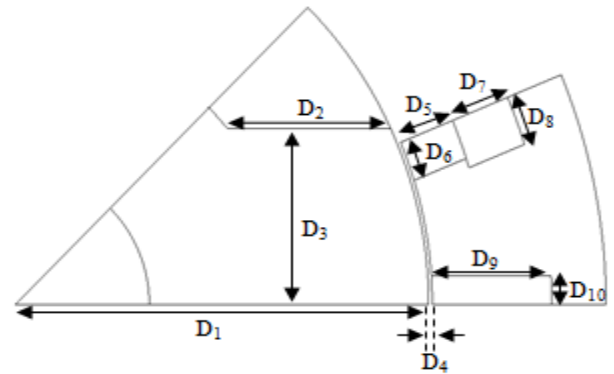


Fig. 3. Motor Design Parameter

### IV. DESIGN PERFORMANCE AND RESULTS BASED ON 2D FINITE ELEMENT ANALYSIS

In this study, 2-D FEA investigation is implemented to examine the impact of various rotor pole numbers on the characteristics of HEFSM in which the number of stator pole is fixed to 8, while the number of rotor pole set to 4, 8, 12, 16 and 20. The flux linkage, the back-emf, cogging torque and average torque are investigated for all topologies.

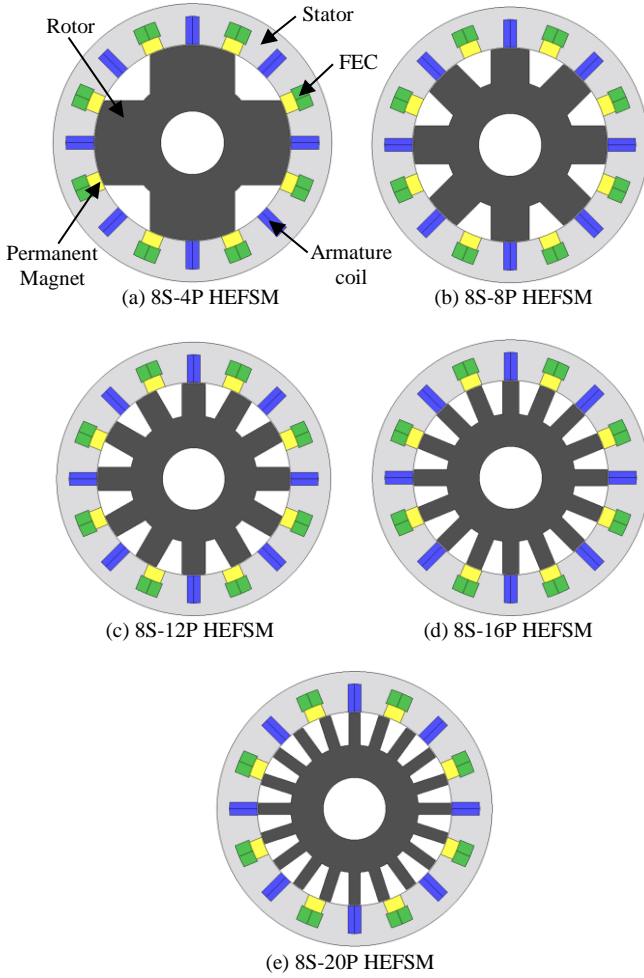


Fig. 4. Preliminary design of the HEFSM configurations

#### A. Flux Linkage of PM and FEC

The Fig. 5 shows the flux interaction of PM with DC FEC for HEFSM. All the flux from PM has been successfully interacts with the FEC flux without any leakage. It is clearly demonstrate that the magnetic flux linkage of 8S-8P HEFSM has the highest amplitude compared with the rest of rotor pole number configurations. This is due to the magnetic flux is easily flow from the stator to the rotor. The amplitude of magnetic flux is reducing with increase in rotor pole number.

#### B. Induced Voltage of PM with DC FEC

The induced voltage of HEFSM at PM with DC FEC only at maximum  $J_E$  of 30 A/mm<sup>2</sup> at various rotor poles is illustrated in Fig. 6. As seen from the graph, 8S-8P has the higher induced voltage follow by 8S-4P. The 8S-20P has less induced voltage generated. This graph show 8S-8P has highest distortion compare to other combination. All the induced voltages are not exceeding the supply voltage which is good for motor performance. If the value of induced voltage exceeds the

supply voltage, the operation of the motors will be interrupt as it is use for regenerative braking to charge battery.

#### C. Cogging Torque

Fig. 7 illustrates the cogging torque profile of PM flux for various rotor poles configurations. Obviously, one cycle cogging torque is formed as the rotor being rotate in a complete 360° electric cycle. It is clear that 8S-16P configuration has highest peak to peak cogging torque and 8S-12P has the lowest peak to peak cogging torque with 1.79mNm and 0.46mNm, respectively. 8S-16P has highest cogging torque due to the effect of high FEC flux linkage flow to the rotor. The cogging torque values produced must not exceed 10% of the average torque because it is unnecessary for the performance of the machine that can produced high vibration and noise.

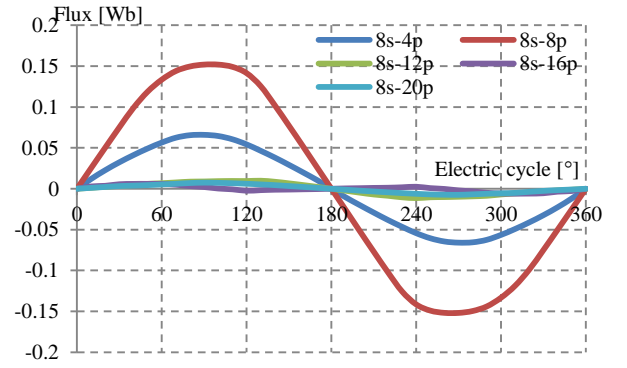


Fig. 5. Flux Linkage of PM with DC FEC with Various  $J_E$

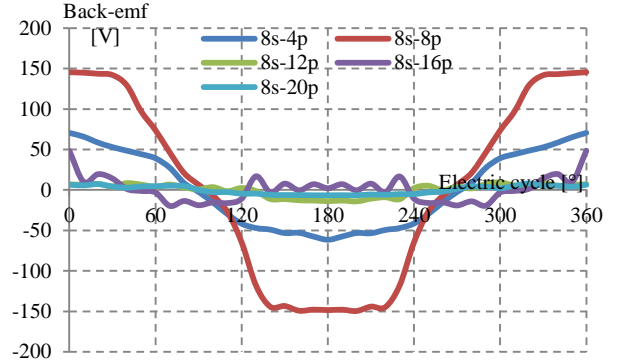


Fig. 7. Induced Voltage of PM with DC FEC



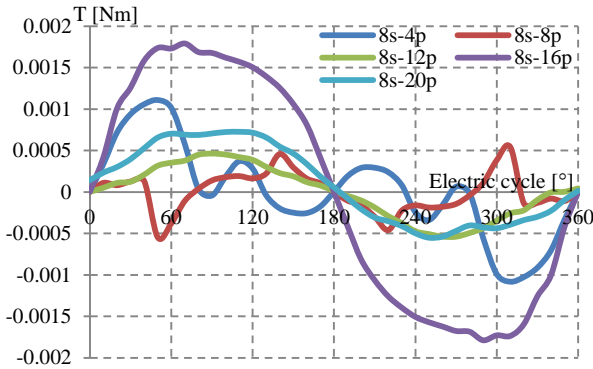
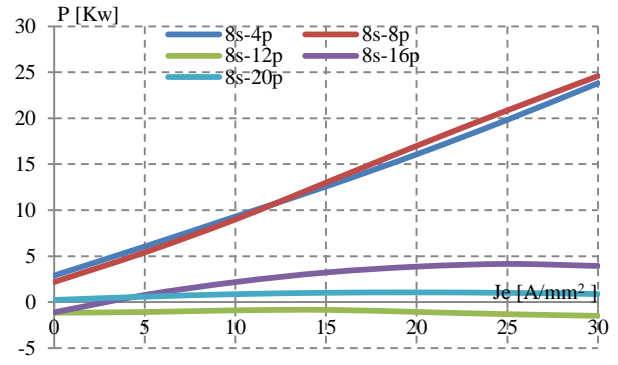


Fig. 8. Cogging Torque of PM Only

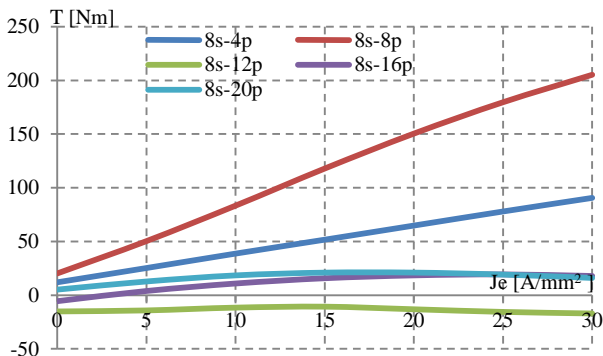
Fig. 10. Power versus  $J_E$  at Maximum  $J_A$ 

#### D. Torque and Power versus FEC Current Density, $J_E$ at Various Armature Coil Current Densities, $J_A$

In In load analysis, both FEC and armature coil current are supplied in the circuit with the values that have been calculated. Both  $J_A$  and  $J_E$  are varied from  $0\text{A/mm}^2$  to  $30\text{A/mm}^2$  and  $0\text{A}_{\text{rms}}/\text{mm}^2$  to  $30\text{A}_{\text{rms}}/\text{mm}^2$ , respectively. Fig. 9 and Fig. 10 show the torque and power versus  $J_E$  at various  $J_A$ , at various rotor poles correspondingly. From the figure, it is shown that the maximum torque and power appears 8S-8P configuration about 205.23Nm and 24.58kW, respectively. For 8S-12P, the output torque and power start to reduce when  $J_E$  is employed. This is due to a lot of magnetic fluxes are cancel with the flux from armature coil and produces negative torque.

#### V. CONCLUSION

In this paper, performance comparison of single-phase inner rotor with various rotor poles has been investigated. 8S-4P and 8S-8P HEFSM are chosen for better performance. The maximum torque achieved for 8S-4P is 90.61Nm which is 81.6% of the target performance; whereas the maximum power has achieved 23.8kW which 58.1% of the target value. Meanwhile, the maximum torque achieves for 8S-8P is 205.23Nm which is already achieves the target performance while maximum power is 24.58Kw which is 60% from the target performance. Although both motor are only the initial design, the torque achieved is considered acceptable and suitable for the single-phase applications. However, design optimization on both HEFSM will be conducted in future.

Fig. 9. Torque versus  $J_E$  at Maximum  $J_A$ 

#### ACKNOWLEDGMENT

This research was supported by GIPS (1369) under Research, Innovation, Commercialization and Consultancy Management (ORICC) UTHM, Batu Pahat and Ministry of Higher Education Malaysia (MOHE).

#### REFERENCES

- [1] M. Z. Ahmad, E. Sulaiman, Z. A. Haron, and T. Kosaka, "Impact of rotor pole number on the characteristics of outer-rotor hybrid excitation flux switching motor for in-wheel drive EV", Proc of Int. Conf on Electrical Eng. & Infor., UKM, pp. 593-601, June 2013.
- [2] M. Z. Ahmad, E. Sulaiman, Z. A. Haron, and T. Kosaka, "Design improvement of a new outer-rotor hybrid excitation flux switching motor for in-wheel drive EV", IEEE Int. Power Engineering and Optimization Conference, Langkawi, pp. 298-303, June 2013.
- [3] M. Z. Ahmad, E. Sulaiman, Z. A. Haron and T. Kosaka, "Preliminary Studies on Permanent Magnet Flux Switching Machine with Hybrid Excitation Flux for Direct Drive Electric Vehicle Application", IEEE Int. Conf. on Power and Energy (PECON-2012), Sabah, pp. 928-933, Dec 2012
- [4] W. Fei, P. Luk, and K. Jinupun, "A New Axial flux magnet segmented-armature-torus machine for in-wheel direct drive applications," IEEE Power Electronics Specialist Conference, pp. 2197-2202, 2008.
- [5] C. C. Chan, "The state of the art of electric, hybrid, and fuel cell vehicles", *Proc. IEEE*, vol. 95, no. 4, pp.704-718, Apr. 2007..
- [6] Jerry Bednarczyk, PE, Induction Motor Theory. Access on November 9, 2012. <http://www.pdonline.org/courses/e176/e176content.pdf>
- [7] C. C. Chan, "The state of the art of electric and hybrid vehicles", *Proc. IEEE*, vol. 90, no. 2, pp. 247-275, Feb. 2002.
- [8] M. Z. Ahmad, E. Sulaiman, Z. A. Haron and T. Kosaka, "A New Structure of Outer-Rotor PMFSM with Hybrid Excitation Flux for In-Wheel Drive EV Applications", Proc. The 5th Int. Conference on Postgraduate Education (ICPE-5 2012), UTM, pp. 531-538, Dec 2012
- [9] S. E. Rauch and L. J. Johnson, "Design principles of flux switch alternators," *AIEE Trans.*, vol 74III, no. 12, pp. 1261-1269, 1955.
- [10] Y. Chen, S. Chen, Z.Q. Zhu, D. Howe, and Y.Y. Ye, "Starting torque of single phase flux switching permanent magnet motors," *IEEE Trans. Magn.*, vol 42, no. 10, pp. 3416-3418, 2006.
- [11] E. Hoang, M. Lecrivain, and M. Gabsi, "A New Structure of a Switching Flux Synchronous Polyphased Machine," in *European Conference on Power Electronics and Applications*, no. 33, pp. 1-8, 2007.
- [12] E. Hoang, A. H. Ben-Ahmed, and J. Lucidarme, "Switching Flux PM Polyphased synchronous machine," in Proc. 7th Eur Conf. Power Electronics Appl., Sept 1997, pp. 903-908.
- [13] Y. Amara, E. Hoang, M. Gabsi, and M. Lecrivain, "Design and comparison of different flux-switching synchronous machines for an aircraft oil breather application," *Euro. Trans Electr. Power*, no. 15, pp. 497-511, 2005.
- [14] M. Z. Ahmad, E. Sulaiman, M. Jenal, W. M. Utomo, et.al, "Design Investigation of Three Phase HEFSM with Outer-Rotor Configuration " *IEEE Conf. on Clean Energy & Technology*, 18-20 Nov 2013

- [15] E. Sulaiman, T. Kosaka, and N. Matsui, "Design Optimization and Performance of a Novel 6- Slot 5-Pole PMFSM with Hybrid Excitation for Hybrid Electric Vehicle", *IEEEJ Transaction on Industry Application*, Vol. 132 / No. 2 / Sec. D pp. 211-218, Jan 2012. (Scopus)
- [16] 29. E. Sulaiman, T. Kosaka, and N. Matsui, "Design and Performance of 6-Slot 5-Pole Permanent Magnet Flux Switching Machine with Hybrid Excitation for Hybrid Electric Vehicle Applications", Proc. The 2010 International Power Electronics Conference, (IPEC 2010), Sapporo (Japan), June 2010.
- [17] E. Sulaiman, T. Kosaka, and N. Matsui, "High power density design of 6S-16P permanent magnet flux switching machine with field excitation for hybrid electric vehicles", *Journal of Power Electronics and Motion Control*, Vol.3, No.1, pp.24-30, Feb 2011.